

Hybrid CSP/PV receivers: Converting optical spillage to electricity

Cite as: AIP Conference Proceedings **2033**, 170006 (2018); <https://doi.org/10.1063/1.5067170>
Published Online: 08 November 2018

Clifford K. Ho, Claiborne O. McPheeters and Paul R. Sharps



View Online



Export Citation

ARTICLES YOU MAY BE INTERESTED IN

[Recent advances in the PV-CSP hybrid solar power technology](#)

AIP Conference Proceedings **1850**, 110006 (2017); <https://doi.org/10.1063/1.4984480>

[Assessment of mid-term growth assumptions and learning rates for comparative studies of CSP and hybrid PV-battery power plants](#)

AIP Conference Proceedings **1850**, 160001 (2017); <https://doi.org/10.1063/1.4984535>

[Integrated techno-economic assessment of hybrid CSP-PV plants](#)

AIP Conference Proceedings **2033**, 180008 (2018); <https://doi.org/10.1063/1.5067180>

Lock-in Amplifiers
up to 600 MHz



Zurich
Instruments



Hybrid CSP/PV Receivers: Converting Optical Spillage to Electricity

Clifford K. Ho,^{1,a)} Claiborne O. McPheeters,^{2,b)} and Paul R. Sharps^{2,c)}

¹Ph.D., Sandia National Laboratories, P.O. Box 5800, MS-1127, Albuquerque, NM 87185-1127, USA

²Ph.D., SolAero Technologies Corp., 10420 Research Rd. SE, Albuquerque, NM 87123

^{a)}Corresponding author: ckho@sandia.gov

^{b)}Clay_McPheeters@solaerotech.com

^{c)}Paul_Sharps@solaerotech.com

Abstract. This paper evaluates a novel receiver design concept that implements photovoltaic (PV) cells on heat shields and bellows shields to capture optical spillage from central receiver and parabolic trough concentrating solar power (CSP) plants, generating electricity from concentrated light that would otherwise be wasted. A combination of conventional silicon and multi-junction concentrating PV (CPV) cells were evaluated to accommodate regions of both high and low solar fluxes on the shields. Estimates from existing CSP plants indicate that the irradiance on central-receiver heat shields can be well over 100 kW/m² near the receiver tubes, but lower fluxes can occur in distant regions or in parabolic trough applications. A technoeconomic study was performed to estimate the levelized cost of energy (LCOE) for these systems as a function of several cost and performance factors, such as irradiance, PV cell type, and cooling conditions.

INTRODUCTION

Optical spillage from heliostats and parabolic trough collectors occurs due to surface aberrations, misalignment, and tracking errors in concentrating solar power (CSP) plants. In central receivers, spillage is accommodated using heat shields fabricated from high-temperature refractory materials above and below the receiver tubes to protect headers and other infrastructure components. In parabolic trough systems, metal bellows shields (collars) spaced several meters apart are used to protect the expansion joints connecting the receiver tubes from concentrated sunlight.

This paper evaluates a novel receiver design concept that implements photovoltaic (PV) cells on these heat shields and bellows shields to generate electricity from concentrated light that would otherwise be wasted (**FIGURE 1**). Das et al. [1] investigated spillage recovery from molten salt central receivers using either feedwater heater panels or concentrated PV (CPV) modules. They assumed a fixed spillage area and average irradiance, along with constant conversion efficiency of the PV modules. In the current work, we investigate the impact of variable irradiance, cell efficiency (as a function of temperature and irradiance), and cooling systems on the system performance and LCOE.

A combination of conventional silicon and multi-junction concentrating PV (CPV) cells were evaluated to accommodate regions of both high and low solar fluxes. Estimates from PHLUX imaging [2] show that the irradiance on central-receiver heat shields can be well over 100 kW/m² near the receiver tubes, but lower fluxes can occur in distant regions or in parabolic trough applications. A technoeconomic study was performed to estimate the levelized cost of energy (LCOE) for these systems as a function of irradiance, PV cell type, and cooling mechanisms.



FIGURE 1. Conceptual design of PV cells on heat shields or standby regions of a central receiver (left) or on the bellows shields of a trough receiver (right).

APPROACH

The PV cell temperature, efficiency, power generation, and LCOE for different hybrid receiver configurations were evaluated using the following procedure:

1. Develop a steady-state heat transfer model using a control volume of the PV cells with consideration of solar irradiance, radiation to the environment, convection to the environment, and energy conversion to electricity (which depends on the PV cell efficiency as a function of temperature and irradiance)
2. Determine the cell temperature that satisfies the steady-state energy balance as a function of irradiance (implicit equation)
3. Determine potential power generation for different receiver configurations and available area*
4. Evaluate costs of components and determine LCOE for PV generation from different hybrid receiver configurations

Analytical heat transfer models were derived to estimate the cell temperature as a function of irradiance and heat transfer coefficients for the application of PV cells on flat heat shields. More detailed computational fluid dynamics models were used to estimate the cooling and heat transfer coefficients associated with finned PV-lined collars that could be used in place of the bellows shields for parabolic trough receivers. Cost and efficiency curves were obtained from literature and from data for silicon and triple-junction PV cells (**FIGURE 2**) and other components such as heat exchangers. Our investigation of CPV cells in hybrid system applications considered both established triple-junction CPV cells, such as the SolAero Concentrating Triple-Junction (CTJ) cell, and next-generation CPV cells that are being developed for high-temperature applications (e.g., up to 400°C per the ARPA-E FOCUS project; <https://arpa-e.energy.gov/?q=arpa-e-programs/focus>). Representative cell efficiencies for silicon ($\eta_{silicon}$) and triple-junction (η_{triple}) cells as a function of irradiance (Q in suns, where 1 sun = 900 W/m²) are provided as follows at a prescribed reference temperature ([3] for silicon cell and SolAero Technologies for triple-junction cell):

$$\eta_{silicon}(25^{\circ}C, Q) = \begin{cases} 2.158 \times 10^{-4} Q^3 - 2.832 \times 10^{-3} Q^2 + 1.246 \times 10^{-2} Q + 0.2089, & \text{if } Q < 6 \text{ suns} \\ -2.269 \times 10^{-5} Q^2 - 1.058 \times 10^{-4} Q + 0.2291, & \text{if } Q \geq 6 \text{ suns} \end{cases} \quad (1)$$

$$\eta_{triple}(10^{\circ}C, Q) = (-5.548 \times 10^{-12} Q^4 + 2.127 \times 10^{-8} Q^3 - 2.965 \times 10^{-5} Q^2 + 1.437 \times 10^{-2} Q + 37.07) / 100 \quad (2)$$

In Eqs. (1) and (2), the cell efficiency is adjusted for cell temperature using the following relation [4]:

$$\eta(T_{cell}, Q) = \eta(T_{ref}, Q) (1 - \beta(T_{cell} - T_{ref})) \quad (3)$$

* At the Ivanpah Solar Electric Generating System (FIGURE 1), over 1000 m² of area is estimated to be available to accommodate PV cells on the heat shields for each of the ~100 MW_e tower units. For a 50 MW_e, parabolic trough plant, nearly 700 m² are estimated to be available on the bellows shields to accommodate PV cells.

where T_{cell} is the actual cell temperature ($^{\circ}\text{C}$), T_{ref} is the reference temperature ($^{\circ}\text{C}$) used in Eqs. (1) and (2), and β is set to 0.001 for silicon [4] and 0.0001 for SolAero's III-V triple-junction cells ([5]). Finally, the cell efficiency is multiplied by 0.8 to get module efficiency from the cell efficiency (based on data from Sunpower [3]). **FIGURE 2** shows the cell efficiency as a function of irradiance and two different temperatures for the silicon and triple-junction cells.

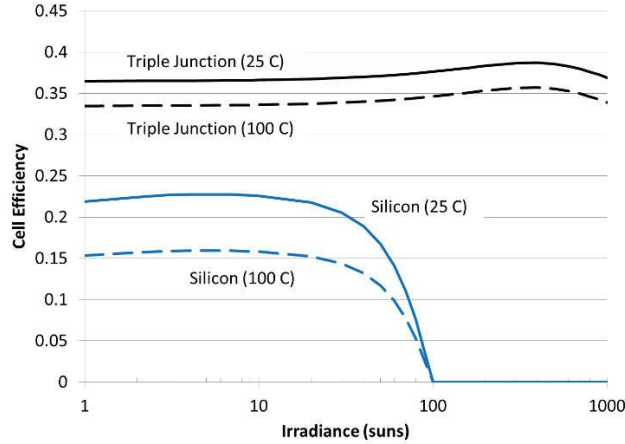


FIGURE 2. Cell efficiency as a function of irradiance and cell temperature (1 sun assumed to be 900 W/m^2).

TABLE 1 summarizes the parameters used in the technoeconomic analyses. The cost of the heat exchanger for central receiver applications is assumed to be a function of the overall heat-exchanger conductance (UA) as reported in [6]. Concepts and designs for back-surface cooling of PV modules is described in Bahaidarah et al. [7].

TABLE 1. Parameters used in the technoeconomic models for different hybrid CSP/PV systems.

Parameter	Tower PV (100 MW _e)	Trough PV (50 MW _e)
Absorptivity / Emissivity	0.9	0.9
Ambient Temperature (K)	300	300
Ratio of module to cell efficiency	0.8	0.8
Available area for PV (m ²) ^a	280	654
Hours of sunlight (hours/year) ^b	4364	4365
Plant availability	0.9	0.9
Hours of sunlight on PV (hours/year)	3930	3930
Cost of module and inverter (\$/m ²) ^c	\$250/m ² (silicon) \$50,000/m ² (triple junction)	\$250/m ² (silicon) \$50,000/m ² (triple junction)
Cost of heat exchanger (\$) ^d	$17.5(\text{UA}(\text{W/K}))^{0.8778}$	$\$2/\text{W}_e$
Number of years for financing	25	25
Interest rate (%) ^e	8%	8%

^aBased on estimated area of heat shields above and below Crescent Dunes receiver (more area available on tower) and 50 MW_e trough plant with annual efficiency of 15%, average DNI of 800 W/m^2 , trough aperture of 5 m, bellows shields spaced every 4 m (0.1 O.D. x 0.3 m), and only the bottom third of the bellows shields being covered by PV cells

^bBased on TMY3 data for Tonopah

^cSilicon PV price from NREL [8] assuming $\sim \$1.5/\text{W}$ (utility-scale, fixed-tilt, projection to 2017) installed and $\sim 170 \text{ W/m}^2$; triple junction price from SolAero Technologies

^dFrom Ho et al. [6], where U is the overall heat transfer coefficient ($\text{W/m}^2\text{-K}$) and A is the heat-transfer area (m²); for troughs, the cost is in $\$/\text{W}_e$ and covers the finned collar and associated costs of installation and retrofitting

^eBased on IEA discount rate used in Technology Roadmap Solar Photovoltaic Energy (2014 edition) [9]

The LCOE is calculated as the annualized costs, A , divided by the annual energy production, where the annual costs are calculated from the total capital costs, C , interest rate, i , and years of financing, n , as follows: $A = C \cdot i(1+i)^n / ((1+i)^n - 1)$.

Modeling

An energy balance was performed on a PV module as shown **FIGURE 3** to determine the cell temperature as a function of irradiance and power losses (heat and electricity).

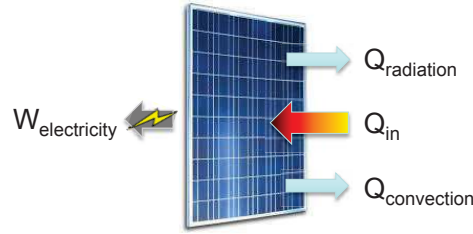


FIGURE 3. Energy balance on PV module to determine cell temperature as a function of irradiance and power losses (heat and electricity).

The energy balance is expressed as follows:

$$\dot{E}_{stored} = \dot{E}_{in} - \dot{E}_{out} - \dot{W}_{out}$$

$$0 = \underbrace{\alpha Q_{in}}_{\text{Absorbed solar radiation}} - \underbrace{h(T_{cell} - T_{\infty})}_{\text{Convective heat loss}} - \underbrace{\varepsilon \sigma (T_{cell}^4 - T_{\infty}^4)}_{\text{Radiative heat loss}} - \underbrace{\alpha Q_{in} \eta(T_{cell}, Q_{in})}_{\text{Electricity production}} \quad (4)$$

where:

- α Solar absorptance (-)
- Q_{in} Solar irradiance (W/m^2)
- h Convection coefficient ($\text{W}/\text{m}^2\text{-K}$)
- T_{cell} Cell temperature (K)
- T_{∞} Ambient temperature (K)
- ε Thermal emissivity (-)
- σ Stefan-Boltzmann constant ($5.67 \times 10^{-8} \text{ W}/\text{m}^2\text{-K}^4$)
- η Cell efficiency expressed as a function of T_{cell} and Q_{in} (**FIGURE 2**)

For the application of PV cells on the heat shields of tower receivers, the impact of different cooling mechanisms and resulting convection coefficients, h , was evaluated. Conditions of passive cooling (natural convection, $h=5 \text{ W}/\text{m}^2\text{-K}$), forced air cooling ($h=100 \text{ W}/\text{m}^2\text{-K}$), and forced liquid cooling ($h=1000 \text{ W}/\text{m}^2\text{-K}$) were investigated, and the impact of these different cooling scenarios on cell temperature, efficiency, annual energy production, and LCOE were determined using the performance parameters shown in **TABLE 1**.

For the application of PV cells on trough bellows shields, computational fluid dynamics (CFD) simulations using Solidworks Flow Simulation were performed to determine average heat transfer coefficients from the finned collars with and without wind (4 m/s). Results showed that the convection coefficient, h , representing heat loss from the finned collar to the ambient under both conditions, was $\sim 100 \text{ W}/\text{m}^2\text{-K}$ (**FIGURE 4**). This value was used for all cases applied to the trough system.

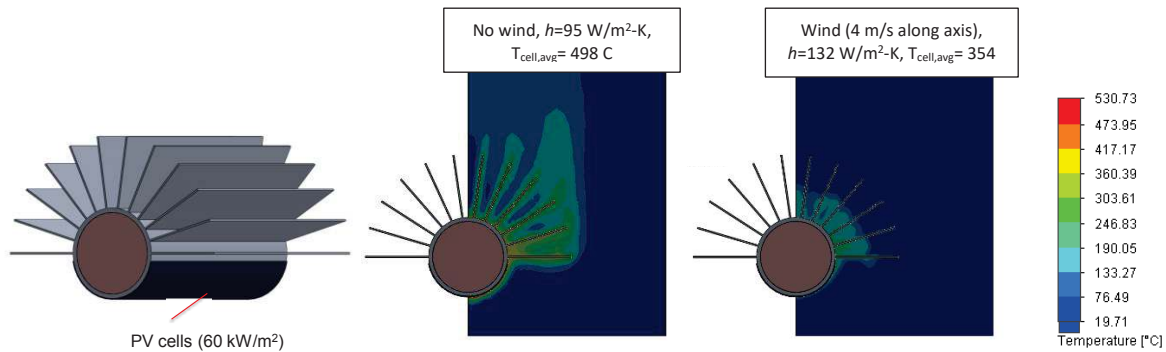


FIGURE 4. CFD simulations of the heat transfer convection coefficient from a finned collar with PV cells on the bottom irradiated at 60 kW/m².

RESULTS

The module efficiency as a function of irradiance for different convection coefficients (cooling mechanisms) is shown in **FIGURE 5** for both triple-junction and silicon cells. Results show that the triple-junction cell yields greater module efficiencies and can withstand higher irradiances. At irradiance levels above 100 suns, the silicon cell efficiency drops to zero. Greater cooling reduces the cell temperature and increases the efficiency in all cases.

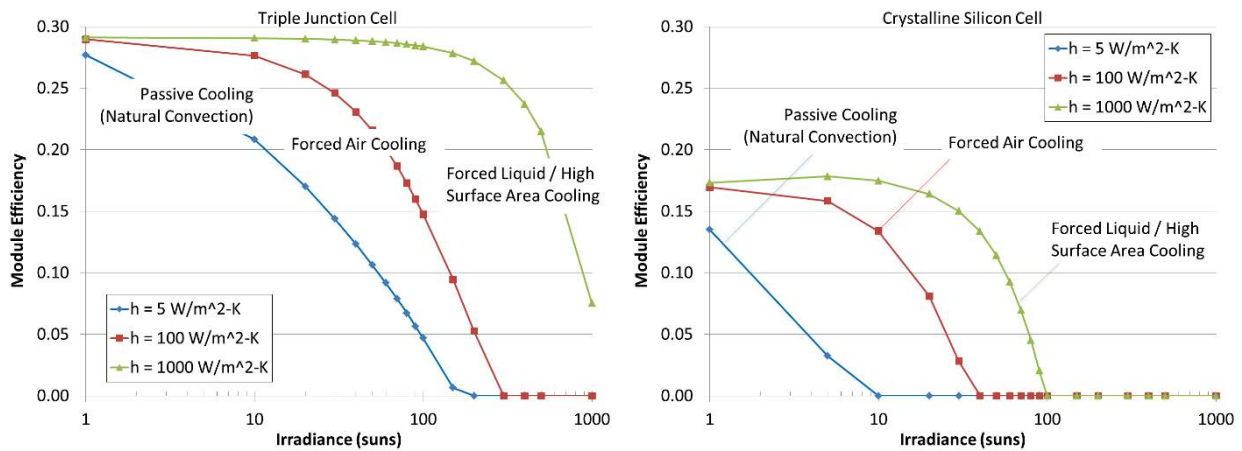


FIGURE 5. Module efficiency of triple junction (left) and crystalline silicon (right) cells as a function of irradiance and cooling (heat transfer coefficients). 1 sun = 900 W/m²

Hybrid Central Receivers

FIGURE 6 shows the annual power generation as a function of irradiance and different cooling conditions from PV modules (triple junction and silicon) placed on the heat shields of a tower receiver using the parameters in **TABLE 1**. For the triple-junction cell, greater cooling yields lower temperatures and increased power generation. For all other cases, there is a maximum power production depending on cooling and irradiance levels. The silicon cells cannot handle high irradiance values, and the power generation peaks at difference irradiance levels (less than 100 W/m²) depending on the cooling mechanism. The power generation from the silicon cells is roughly an order of magnitude less than from the triple-junction cells.

FIGURE 7 shows the estimated LCOE of the PV generation as a function of irradiance and cooling mechanisms for both the triple-junction and silicon cells. Results show that with passive cooling, a clear minimum exists at ~60 – 80 suns for the triple-junction cell, but the LCOE is quite high at ~\$0.20/kWh. With active cooling, the LCOE drops to less than \$0.10/kWh as the benefits of lower temperatures and higher cell efficiencies outweighs the additional costs of the cooling system (the active cooling system could also be used to preheat the heat-transfer media, which

was not considered in this study). For conventional silicon PV cells, results show that minimum LCOE values were achieved at relatively lower irradiances due to lower cell efficiencies. It is proposed that silicon PV cells be used in regions of lower irradiance ($\sim 10 - 50 \text{ kW/m}^2$), and multi-junction cells with active cooling be used in higher irradiance regions to yield the lowest LCOE values for hybrid CSP/PV tower receiver configurations.

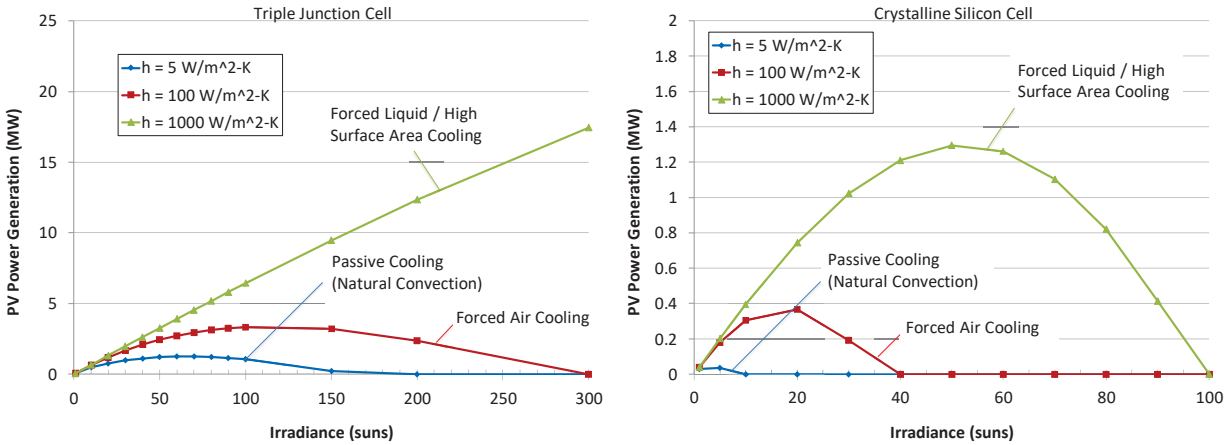


FIGURE 6. PV power generation as a function of irradiance and cooling mechanisms for triple-junction (left) and crystalline silicon (right) cells applied to heat shields of a $\sim 100 \text{ MW}_e$ central receiver CSP plant.

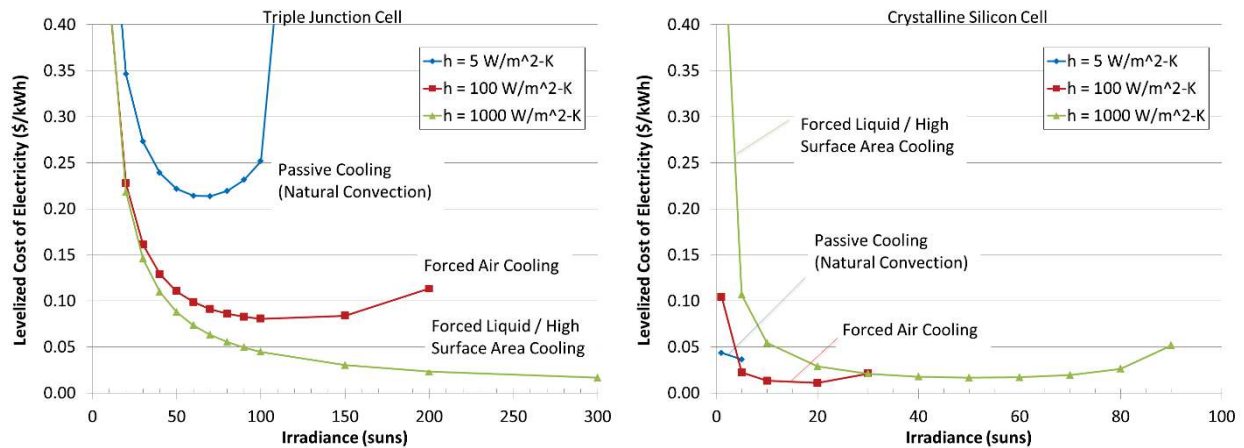


FIGURE 7. Levelized cost of energy as a function of irradiance and cooling mechanisms for triple-junction (left) and crystalline silicon (right) cells applied to heat shields of a $\sim 100 \text{ MW}$ central receiver CSP plant.

Hybrid Parabolic Trough Receivers

FIGURE 8 shows the annual power generation and LCOE for triple-junction and silicon PV cells placed on the bellows shields of a 50 MW_e parabolic trough plant. Results show that the power generation from triple-junction cells is significantly larger than from the silicon cells, but the LCOE is also significantly higher (above $\sim \$0.15/\text{kWh}$). The silicon cells only produce power for irradiance levels less than ~ 40 suns for the prescribed heat transfer convection coefficient of $100 \text{ W/m}^2\text{-K}$, but the LCOE drops to $\sim \$0.05/\text{kWh}$. These results indicate that the use of conventional silicon cells may be more appropriate for the trough applications since the irradiance levels are low compared to the tower applications. The additional cost of the triple-junction cells are not offset by the increased efficiencies at higher irradiance levels.

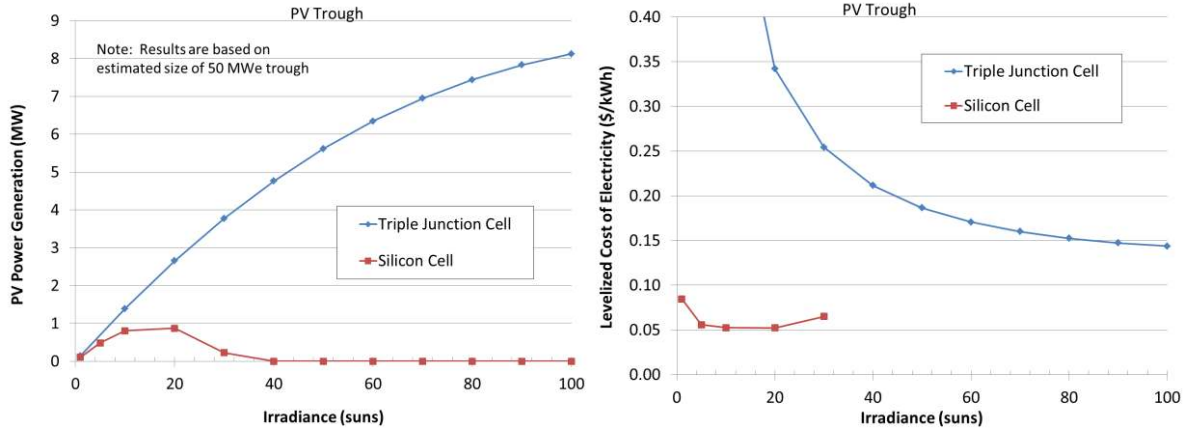


FIGURE 8. Annual power generation (left) and LCOE (right) for PV cells placed on bellows shields in a 50 MWe parabolic trough plant. The convection coefficient, h , was assumed to be 100 W/m²-K for all cases (**FIGURE 4**).

For both the central-receiver and parabolic-trough hybrid CSP/PV applications, a significant challenge is the non-uniform irradiance distribution on the PV cells. Non-uniform fluxes can negatively impact performance of the PV array. The use of microinverters may help mitigate non-uniform flux distributions, but they cost significantly more than central inverters. Another potential issue is the production of glare from the surface of PV modules, especially if they are placed on top of the tower [10, 11]. Specular reflections from the glass surface of the module may cause glare to pilots flying nearby. However, as opposed to direct specular reflections from heliostats, the reflections from the PV modules will be reduced significantly due to the low reflectance of the PV cover glass [12].

CONCLUSIONS

This paper provided a technoeconomic evaluation of a hybrid receiver design for CSP plants that utilizes PV cells to capture optical spillage on heat shields and bellows shields at central receiver and parabolic trough plants, respectively. Both III-V multi-junction and single-junction silicon cells were evaluated. Results showed that with passive cooling of triple junction cells, a minimum LCOE exists at ~60 – 80 suns for a 100 MWe central receiver, but the LCOE was quite high at ~\$0.20/kWh. With active cooling, the LCOE dropped to less than \$0.05/kWh as the benefits of lower temperatures and higher cell efficiencies outweighed the additional costs of the cooling system, and the annual power generation could exceed 10 MW, or 10% of the CSP plant capacity. With conventional silicon PV cells on central receiver heat shields, the minimum LCOE values of less than \$0.05/kWh were achieved at relatively lower irradiances (<100 W/m²) due to lower cell efficiencies. For parabolic trough applications, the triple-junction cells were not cost-effective at the lower irradiance levels of the trough applications. Silicon PV cells yielded LCOE values less than \$0.05/kWh, but the annual power generation was only up to ~1 MW, or 2% of the trough CSP plant capacity. In general, it is proposed that silicon PV cells can be used in spillage regions of lower irradiance (~10 – 50 kW/m²), and multi-junction cells with active cooling be used in higher irradiance regions (for central receiver applications) to yield the lowest LCOE values for hybrid CSP/PV receiver configurations. Issues and challenges associated with hybrid CSP/PV technologies include non-uniform irradiances on the PV cells and potential glare from the reflected concentrated sunlight.

ACKNOWLEDGMENTS

The work conducted by Sandia was funded by Strategic Partnership Projects #061150121 with SolAero Technologies Corp. SolAero was funded under contract with Yale (C15E11945(E00158)) through the ARPA-E FOCUS Solar Cell Development Project. Sandia National Laboratories is a multimission laboratory managed and operated by National Technology and Engineering Solutions of Sandia, LLC., a wholly owned subsidiary of Honeywell International, Inc., for the U.S. Department of Energy’s National Nuclear Security Administration under contract DE-NA0003525.

REFERENCES

1. A. K. Das, P. Inigo, J. D. McGrane, R. J. Terdalkar and M. M. Clark, *Design concepts for spillage recovery in a molten salt central receiver*, *J Renew Sustain Ener* **9** (2) (2017).
2. C. K. Ho and S. S. Khalsa, *A Photographic Flux Mapping Method for Concentrating Solar Collectors and Receivers*, *J Sol Energ-T Asme* **134** (4) (2012).
3. Z. S. Judkins, K. W. Johnston, C. Almy, R. J. Linderman, B. Wres, N. A. Barton, M. Dawson and J. Peurach, *Performance Results of a Low-Concentration Photovoltaic System Based on High Efficiency Back Contact Cells*, 2010.
4. E. Skoplaki and J. A. Palyvos, *On the temperature dependence of photovoltaic module electrical performance: A review of efficiency/power correlations*, *Sol Energy* **83** (5), 614-624 (2009).
5. SolAero Technologies Corp., *CTJ Photovoltaic Cell High Efficiency Triple-Junction Solar Cell for Terrestrial Applications*, 2015.
6. C. K. Ho, M. Carlson, P. Garg and P. Kumar, *Technoeconomic Analysis of Alternative Solarized s-CO₂ Brayton Cycle Configurations*, *J. Solar Energy Engineering* **138**, 051008-051001 (2016).
7. H. Bahaidarah, A. Subhan, P. Gandhidasan and S. Rehman, *Performance evaluation of a PV (photovoltaic) module by back surface water cooling for hot climatic conditions*, *Energy* **59**, 445-453 (2013).
8. D. Chung, C. Davidson, R. Fu, K. Ardani and R. Margolis, *U.S. Photovoltaic Prices and Cost Breakdowns: Q1 2015 Benchmarks for Residential, Commercial, and Utility-Scale Systems*, Report No. NREL/TP-6A20-64746, 2015.
9. International Energy Agency, *Technology Roadmap Solar Photovoltaic Energy*, 2014.
10. C. K. Ho, in *Solar Today* (American Solar Energy Society, Boulder, CO, 2013), pp. 28 - 31.
11. C. K. Ho, C. A. Sims and J. M. Christian, *Evaluation of glare at the Ivanpah Solar Electric Generating System*, International Conference on Concentrating Solar Power and Chemical Energy Systems, Solarpaces 2014 **69**, 1296-1305 (2015).
12. J. Yellowhair and C. K. Ho, *Assessment of Photovoltaic Surface Texturing on Transmittance Effects and Glint/Glare Impacts*, in *Proceedings of the ASME 2015 Power and Energy Conversion Conference*, San Diego, June 28 - July 2, 2015.